Energy Optimal Tracking Control with Discrete Fluid Power Systems using Model Predictive Control

Anders H. Hansen, Magnus F. Asmussen and Michael M. Bech
Department of Energy Technology,
Aalborg University
Pontoppidanstraede 111
E-mail: ahh@et.aau.dk

ABSTRACT

For Discrete Displacement Cylinder (DDC) drives the control task lies in choosing force level. Hence, which force level to apply and thereby which pressure level each cylinder chambers shall be connected to. The DDC system is inherently a force system why often a force reference is generated by a tracking controller and translated into a discrete force level in a Force Shifting Algorithm (FSA). In the current paper the tracking controller and the FSA are combined in a Model Predictive Control algorithm solving the tracking problem while minimizing the energy use. Two MPC algorithms are investigated and compared to a PID like tracking controller combined with a FSA. The results indicate that the energy efficiency of position tracking DDC systems may be improved significantly by using the MPC algorithm.

KEYWORDS: Fluid Power, Digital Displacement, Model Predictive Control

1 INSTRUCTION

Digital hydraulics as a technology is claimed to enable energy efficient and robust systems compared to classical fluid power systems. The use of on/off valves allows a flexible system architecture where control volume pressures are controlled individually and not two and two depending on the same spool valve.

Three main categories within Digital fluid powered cylinder-valve drives are; systems based on Digital Flow Control Unit, systems based on Discrete Displacement Cylinder or systems based on Pulse Width Modulated valves. All of which have system architectural advantages when compared to traditional 4/3 way valve-cylinder drives with respect to energy efficiency.

This paper focuses on a Discrete Displacement Cylinder (DDC) i.e. is a cylinder with a number of working chambers which may be connected to a number of fixed pressure level supply lines. These systems are sometimes referred to as secondary control cylinders. As the cylinder chambers are connected to the pressure lines through "large" on/off valves throttling losses are small and indeed the throttling is not used for control. The DDC is a force system with a discrete number of applicable force levels generated by connecting the cylinder chambers to the fixed pressure level supply lines. A sketch of such system is seen in Fig. 1.

Earlier research have investigated the system architecture and component control and requirements, see e.g. [1, 2, 3, 4, 5, 6]. In [3] energy losses in connection to force shifts were investigated.

The current work investigates the control of DDC's with focus on the energy usages. Hence, a control algorithm performing an energy efficient position tracking is developed. The discrete nature of the DDC system induces many solutions for the same tracking problem. In [1] the choice to shift force or not and which to shift to is made based on minimising a cost function weighing the force error and if a valve change is made. In [2] a cost function weighing the force error against a weighted chamber pressure change is used, i.e. the idea was to limit the energy loss due to force shifting. In both [1, 2] the force reference is generated from a classical linear tracking controller and hence, the force reference is continuous and do not include knowledge of the discrete force system.

In the current paper, a Model Predictive Controller will be designed for energy optimal tracking control. Hence, the tracking control algorithm includes knowledge of the discrete force system. Two MPC strategies will be developed and compared by simulations. Furthermore, a classical PID tracking controller will be designed as benchmark.

In the next section the case system will be presented and modelled, furthermore the MPC structure and objective function will be introduced as well as the PID controller. The section ends by presenting the test trajectory for the simulation model. In the third section the simulation results for the MPC and PID controllers are investigated. Also, the influence of the prediction horizon and step time will be shown. The section concludes by comparing the two MPC strategies with the PID strategy. In the Discussion section the feasibility of DDC in tracking systems is considered in terms of force shifting time and force resolution in comparison to the load system. Furthermore, the required model complexity for the MPC algorithm is discussed as well as the MPC calculation time.

2 METHOD

The feasibility of MPC for discrete fluid power secondary control is in this paper investigated in a simulation study. Hence, a large inertia system is driven with a discrete fluid power force system. The DDC system consists of a three chamber cylinder connected to three pressure lines through nine on/off valves. A MPC strategy is setup to fulfil the tracking requirement while keeping the energy usage low. The derived MPC strategy will be compared to traditional PID feedback tracking control where the choice of discrete force level is done by a Force Shifting Algorithm.

2.1 System Model

The load system is a simple mass-spring-damper system as shown in figure 1. The DDC system used is the one investigated in [7, 8]. As seen in figure 1 it consists of a three chamber cylinder which through on/off valves may be connected to three pressure lines. The pressures in the supply lines are assumed constant.

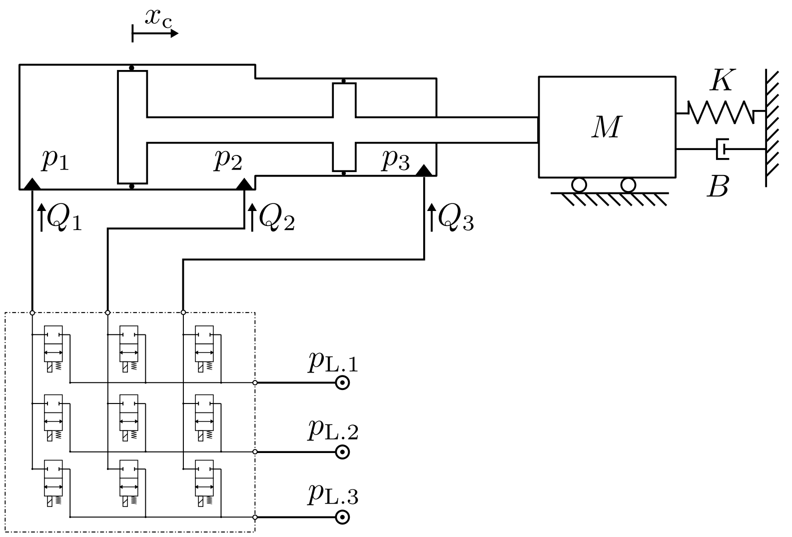

Figure 1: DDC force system and the load system.

The dynamic equation for the load system reads:

$$M\ddot{x}_c(t) + B\dot{x}_c(t) + Kx_c(t) = f_c(t) \tag{1}$$

where the force from the DDC is $f_c(t)$. The actuator model consists of three continuity equation on the format (3), one for each cylinder chamber and an orifice equation for each on/off valve. [9].

$$f_c(t) = \Sigma_{i=1}^{3} A_i p_1(t) \tag{2}$$

$$\dot{p}_i(t) = \frac{\beta_i}{V_i(x_c)} \left(Q_i(t) + A_i \dot{x}_c(t)\right) \tag{3}$$

$$Q_i(t) = \Sigma_{j=1}^{3} k_v u_{i,j} \sqrt{|p_{L,j} - p_i|} \mathrm{sign}(p_{L,j} - p_i) \tag{4}$$

$p_{L,j}$ is the pressure in the j'th supply line and $u_{i,j}$ is the valve state for the valve connecting the i'th cylinder chamber with the j'th supply line. k_v is the valve coefficient for the on/off valves. The hose connection from the valve manifold to the cylinder chambers are assumed short compared to the system dynamics and hence left unmodelled.

With the system layout given in Tab. 1 the force vector and the according steady state positions are given in Fig. 2.

$M = 660 \cdot 10^3$ kg	$A_1 = (+)235$ cm^2	$p_{L.1} = 20$ bar
$B = 215 \cdot 10^3$ N/s	$A_2 = (-)122$ cm^2	$p_{L.2} = 100$ bar
$K = 2513$ kN	$A_3 = (-)87$ cm^2	$p_{L.3} = 180$ bar

Table 1: System parameters for the load and the fluid power systems, based on [8].

For each of the applicable forces seen left in Fig. 2 a corresponding piston position is seen to the right. Hence, the position given in the right plot may be obtained with a constant force value from the applicable force vector.

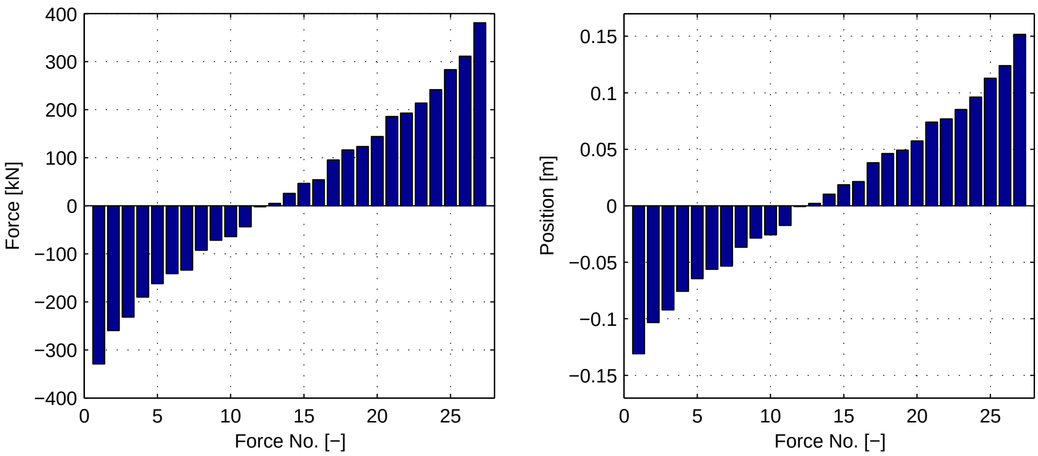

Figure 2: Applicable force vector and according steady state positions.

2.2 Control Strategy

The driving system is by nature a force system. Hence, given a valve input matrix **u** the cylinder produces a given force. The output of the controller is therefore a force reference. The PID like feedback controller will generate a continuous force reference which must be translated to a discrete force value by a FSA. The MPC is formulated as an integer problem such it directly chooses one of the available force levels. In each controller time step, T_s, the MPC algorithm runs an optimisation that finds a vector of force levels minimising the object function over a given prediction horizon, $T_\mathrm{H} = T_\mathrm{s}N$. Hence, the MPC finds the force level to be applied into the future, $[F(T_\mathrm{s})\ F(2T_\mathrm{s})\ F(3T_\mathrm{s})\ ..\ F(NT_\mathrm{s})]$. The controller however only input $F(T_\mathrm{s})$ after which a new vector of forces is calculated.

2.2.1 MPC

The tracking problem is solved with two strategies MPC_1 and MPC_2. Firstly the tracking error and the energy losses are combined in an objective function (5). Secondly, the objective function (6) only holds the energy losses while a constraint on the tracking error is included in (8).

$$J_1 = \frac{W_1}{T_\mathrm{H}}\left(\Sigma_{n=1}^{N} E_\beta(n) + \int_0^{T_\mathrm{H}} E_\mathrm{t}(t)dt\right) + \frac{1}{T_\mathrm{H}}\int_0^{T_\mathrm{H}} W_2 e_\mathrm{c}(t)^2 + \dot{e}_\mathrm{c}(t)^2 dt \tag{5}$$

$$J_2 = \frac{1}{T_\mathrm{H}}\left(\Sigma_{n=1}^{N} E_\beta(n) + \int_0^{T_\mathrm{H}} E_\mathrm{t}(t)dt\right) \tag{6}$$

The energy losses included in the objective functions are losses induced during force shifting E_β and throttling losses E_t across the on/off valves. The MPC_1 algorithm is tuned using the weighing parameters W_1..

The optimal force level in the time horizon T_H is k^+, i.e. a vector holding the optimal forces at time $t = T_\mathrm{s}k$ for $k = 1,\ 2...\ N$ and is found as

$$k^+ = \arg\min_{k\in S}\{J_1\} \tag{7}$$

$$k^+ = \arg\min_{k\in S}\{J_2|\ \ |e_\mathrm{c}(t)| < \delta\} \tag{8}$$

for MPC_1 and MPC_2 respectively. The elements for the solution k^+ must belong to the S which is the set of available forces, here the integers from 1 to 27. Note, that MPC_2 is tuned with the error measure δ contrary to some weighing parameters.

The derivative of the error is included in the objective function as a consequence of observed instability for a cost function only minimising the error. Proof of stability for the formulated MPC is not directly addressed in this work, but only handled through tuning of weight factors W_1 and W_2.

The model used for the MPC formulation is the dynamic equation of the load system represented in state space:

$$\begin{aligned} \dot{x} &= A_\mathrm{c} x + B_\mathrm{c} u \\ y_k &= C_\mathrm{c} x \end{aligned} \tag{9}$$

where the system matrices for the continuous system is:

$$A_\mathrm{c} = \begin{bmatrix} 0 & 1 \\ \frac{-K}{M} & \frac{-B}{M} \end{bmatrix} , \quad B_\mathrm{c} \begin{bmatrix} 0 \\ \frac{1}{M} \end{bmatrix} , \quad C_\mathrm{c} \begin{bmatrix} 1 & 0 \end{bmatrix} \tag{10}$$

Note, that in MPC the input u is discrete in time with constant sample time T_s, i.e. the input may be seen as a comming from a zero-order hold. A discrete representation of the system model may be formulated:

$$\begin{aligned} x_{k+1} &= A x_k + B u_k \\ y_k &= C x_k \end{aligned} \tag{11}$$

By recursive evaluation of the discrete state space model future system states may be described by:

$$\underbrace{\begin{bmatrix} x_{k+1} \\ x_{k+2} \\ x_{k+3} \\ \vdots \\ x_{k+N} \end{bmatrix}}_{x_{k+}} = \underbrace{\begin{bmatrix} A \\ A^2 \\ A^3 \\ \vdots \\ A^N \end{bmatrix}}_{P} x_k + \underbrace{\begin{bmatrix} B & 0 & 0 & \cdots & 0 \\ AB & B & 0 & \cdots & 0 \\ A^B & AB & B & \cdots & 0 \\ \vdots & \vdots & \vdots & \ddots & \vdots \\ A^{N-1}B & A^{N-2}B & A^{N-3}B & \cdots & B \end{bmatrix}}_{H} \underbrace{\begin{bmatrix} u_k \\ u_{k+1} \\ u_{k+2} \\ \vdots \\ u_{k+N-1} \end{bmatrix}}_{u_{k+}} \tag{12}$$

The future system output, i.e. the future cylinder position, may be described as:

$$y_{k+} = C_x x_{k+}, \qquad C_x = \begin{bmatrix} C & 0 & 0 & \cdots & 0 \\ 0 & C & 0 & \cdots & 0 \\ 0 & 0 & C & \cdots & 0 \\ \vdots & \vdots & \vdots & \ddots & \vdots \\ 0 & 0 & 0 & \cdots & C \end{bmatrix} \tag{13}$$

The squared error and derivative of error over the time horizon of the objective function (5) may then be approximated by a static algebraic problem:

$$\int_0^{T_\mathrm{H}} W_2 e_\mathrm{c}(t)^2 + \dot{e}_\mathrm{c}(t)^2 dt \approx \left(x_{\mathrm{c,ref}+} - P x_k - H u_{k+}\right)^T Q \left(x_{\mathrm{c,ref}+} - P x_k - H u_{k+}\right) \tag{14}$$

where $x_{\mathrm{c,ref+}}$ is a vector containing position and velocity references at time $t = kT_\mathrm{s}$ for $k = 1,\ 2\ \ldots\ N$ and Q a diagonal matrix with $\begin{bmatrix} W_2 & 0 \\ 0 & 1 \end{bmatrix}$. Two actuator energy losses are included in the objective functions (5) and (6). The first energy loss is associated with changing the pressure in the cylinder chambers which is calculated by:

$$E_\beta = \frac{1}{2}\Delta p^2 \frac{V}{\beta} \tag{15}$$

The total shifting loss over the time horizon may then be calculated for both cost functions:

$$\Sigma_{n=1}^{N} E_\beta(n) = \Sigma_{n=1}^{N}\Sigma_{i=1}^{3}\frac{1}{2}\left(p_i(n) - p_i(n-1)\right)^2 \frac{V}{\beta} \tag{16}$$

where $p_i(n)$ denotes the pressure in the i'th chamber corresponding to the force level at step n.

The second loss is the throttling loss in the valve manifold. Which is calculated by the piston velocity and a loss coefficient $k_\mathrm{t} = \Sigma_{i=1}^{3}\frac{A_i^3}{k_{\mathrm{v},i}^2}$. The total throttling loss during a prediction horizon T_H is given by:

$$\int_0^{T_\mathrm{H}} E_\mathrm{t}(t)dt \approx \Sigma_{k=1}^{N}|\dot{x}_\mathrm{c}(k)^3 k_\mathrm{t}| \tag{17}$$

where $\dot{x}_\mathrm{c}(k)$ is calculated in the same manner as (13) with $C = \begin{bmatrix} 0 & 1 \end{bmatrix}$.

The optimisation problem of both MPC formulations is in this work solved by a differential evolution algorithm, see e.g. [10].

2.2.2 PID Feedback

The load system plant is the linear second order system given as:

$$G_\mathrm{p}(s) = \frac{X_\mathrm{c}(s)}{F_\mathrm{c}(s)} = \frac{1}{Ms^2 + Bs + K} \tag{18}$$

for which a bode plot and a step response are seen in Fig. 3.

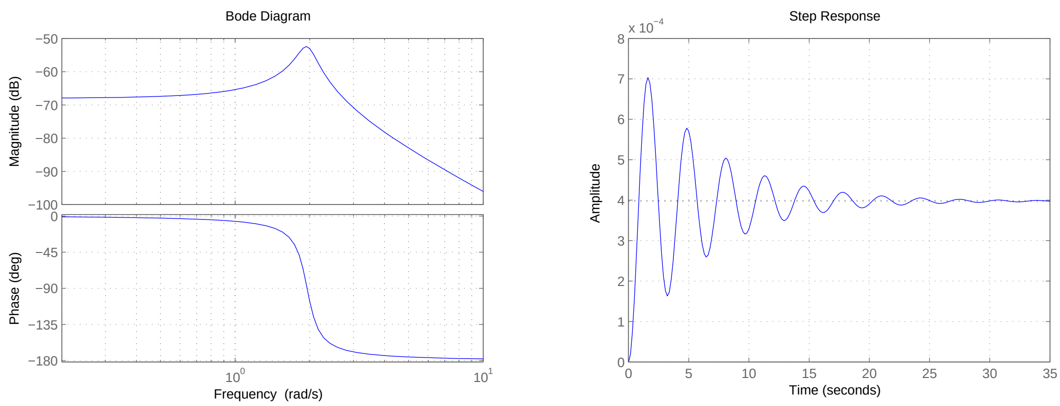

Figure 3: Bode diagram and step response of the load system, $G_\mathrm{p}(s)$.

A PID-like controller is designed for position tracking:

$$G_{\mathrm{c}}(s) = K_{\mathrm{c}} \left(K_{\mathrm{p}} s + \frac{K_{\mathrm{i}}}{s} + \frac{K_{\mathrm{d}} s}{\tau_{\mathrm{d}} s + 1} \right) \tag{19}$$

In the control design phase the force system is approximated by a first order system resembling the pressure build up in a constant volume through a fixed orifice:

$$G_{\mathrm{f}}(s) = \frac{F_{\mathrm{c}}(s)}{F_{\mathrm{c.ref}}(s)} = \frac{1}{\tau_{\mathrm{f}} s + 1} \tag{20}$$

The combined actuator and plant then becomes a third order system consisting of a "slow" second and a "faster" first order system. The bode plot of the normalised system is seen in Fig. 4 (a). The controller designed is seen in Fig. 4 (b).

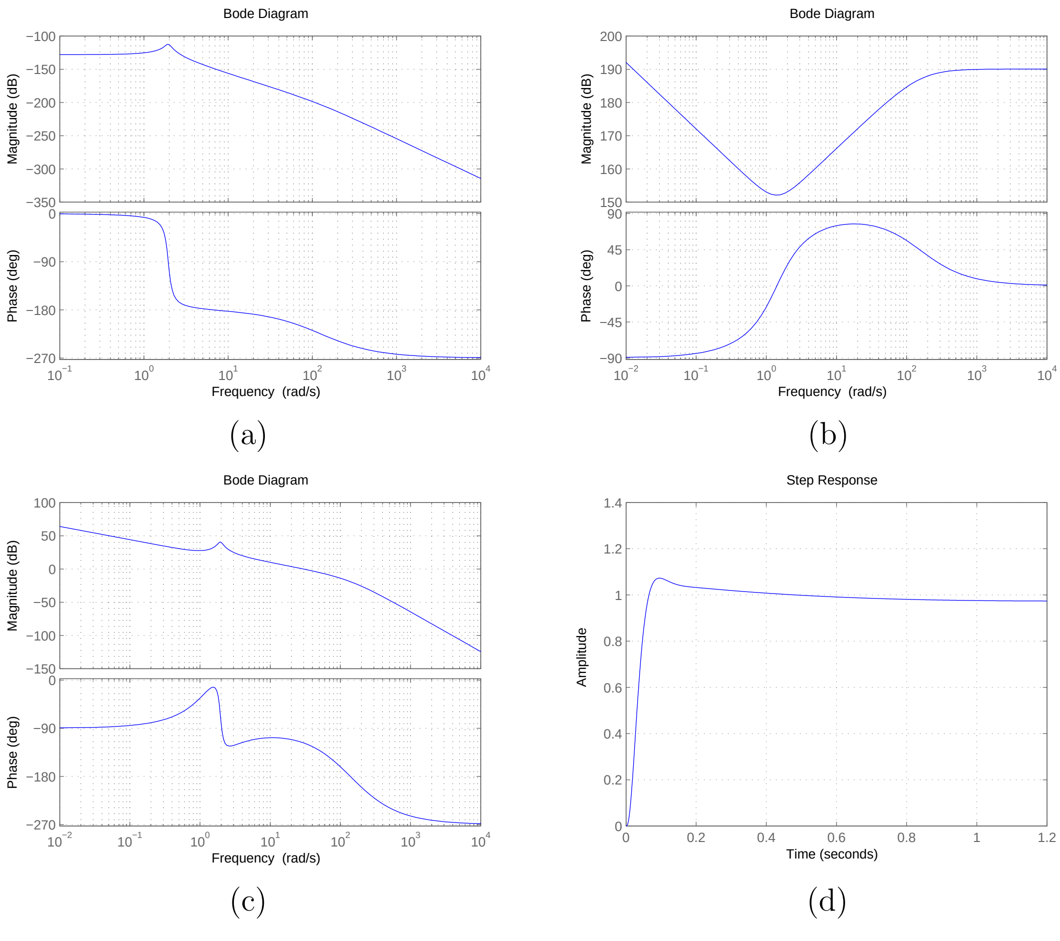

Figure 4: (a) Uncontrolled system with force dynamic approximations. (b) The applied controller. (c) Controlled open loop system. (d) Closed loop step response.

A bode diagram of the open loop controlled system is seen in Fig. 4 (c) and a closed loop position step response of the controlled system is seen in Fig. 4 (d). The controller constants employed are given in Tab. 2.

$K_{\mathrm{c}} = 40 \cdot 10^6$	$K_{\mathrm{p}} = 1$	$K_{\mathrm{i}} = 1$	$K_{\mathrm{d}} = 0.5$	$\tau_{\mathrm{d}} = 0.064$

Table 2: Controller constants for (19).

2.2.3 Force Shifting Algorithm

Using a discrete force system entails that the applied force must be chosen between the force levels available. Therefore, a translation from the continuous controller output to force level is required. This translation is conducted with a FSA. The FSA is developed to weigh the energy loss associated with a given force shift against the force error:

$$k = \arg\min_{k \in S} \{ |f_{\text{c.ref}}(t) - F_{\text{c}}(k)| + W_4 E_\beta(k) \} \tag{21}$$

The FSA updates the output reference every T_{s}. W_4 is a tuning parameter left for trade-off between tracking performance and energy use.

2.3 Test Trajectory

When performing tests of the position controllers a feasible input reference is required. Hence, the system is tested against a reference with transient changes within the system limits. The position trajectory is defined as a piece-wise function of 5'th order polynomials given as:

$$x(t) = a_5 t^5 + a_4 t^4 + a_3 t^3 + a_2 t^2 + a_1 t + a_0 \tag{22}$$

In this work, the initial and end velocity and accelerations are is set to zero. Hence, the polynomial constants are depending on the time duration of the movement, the start and end position and simplifies to the generic constants:

$$\begin{aligned} a_0 = x(0) \quad a_1 = 0 \quad a_2 = 0 \quad a_3 &= \frac{1}{2T^3}\left(20(x(T) - x(0))\right) \\ a_4 = \frac{1}{2T^4}\left(30(x(0) - x(T))\right) \quad a_5 &= \frac{1}{2T^5}\left(12(x(T) - x(0))\right) \end{aligned} \tag{23}$$

The total test trajectory used is seen in Fig. 5.

As seen the input trajectory is made such the piston is moved to various positions and held still. This enables testing of both steady state and transient performance.

3 RESULTS

To see the importance of the parameters T_{s} and T_{H} for the MPC, results of a parameter study is shown in Fig. 6. The influence of each parameter is isolated by setting $W_1 = 0$ such that only the tracking error is minimised. To further simplify the parameter study the actuator dynamics are neglected, i.e. an ideal discrete force system is assumed. For the time horizon sweep the step time is set to 0.1s whereas the time horizon is set to 1s for the time step sweep. The performance is evaluated on the mean squared error and the mean used power given in respectively (24) and (25).

$$e_{\text{mse}} = \frac{1}{T} \int_0^T (x_{\text{c,ref}}(t) - x_{\text{c}}(t))^2 dt \tag{24}$$

$$P_{\text{used}} = \frac{1}{T} \int_0^T \Sigma_{j=1}^3 \Sigma_{i=1}^3 Q_{i,j}(t) p_{\text{L},j} dt \tag{25}$$

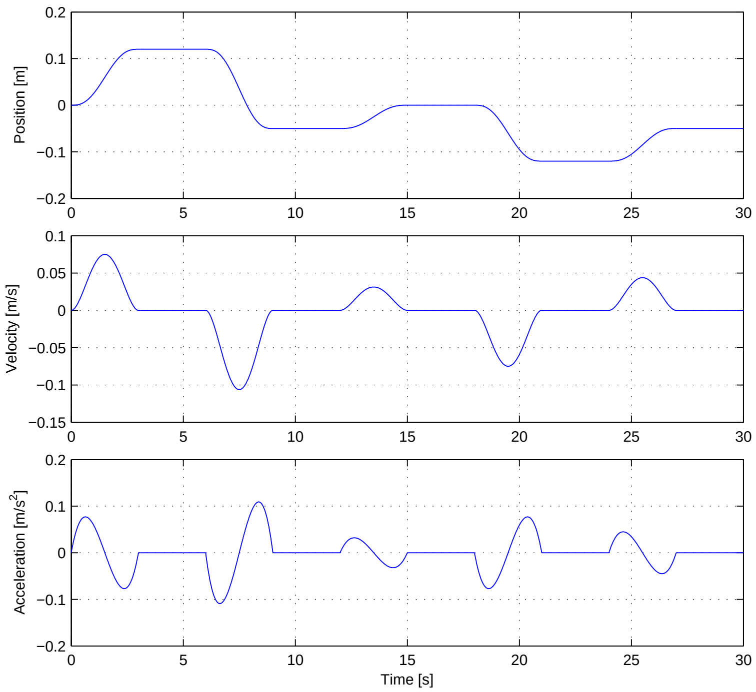

Figure 5: Plot of the input reference trajectory for the cylinder position.

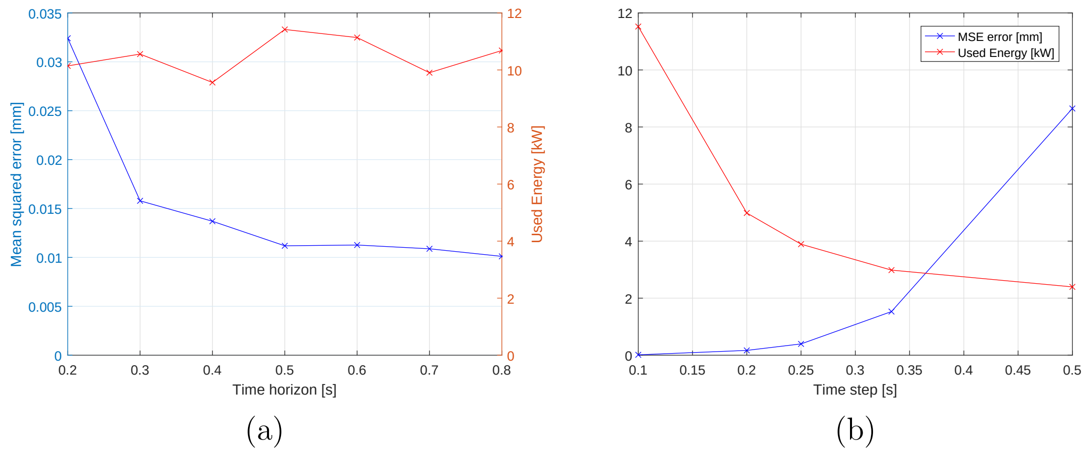

Figure 6: Energy and mean squared error for various time step and horizon length.

Where $Q_{i,j}$ is the flow from the i'th cylinder chamber to the j'th supply line.

From Fig. 6(a) it may be seen that the mean squared tracking error decreases with an increasing time horizon of the MPC. Increasing the time horizon above approximately 0.5s does not result in a lower mean squared tracking error.

In Fig. 6(b) it is shown that the mean squared tracking error increases with an increasing step time of the MPC. In addition it may be seen that the consumed energy over the trajectory decreases with the increasing step time of the MPC due to fewer force shifts.

In Fig. 7(a) a parameter study of the weight, W_1, in (5) is shown. As seen the used energy decreases with the increase in weight on the used energy while the mean squared tracking error increases. In Fig. 7(b) a study of the maximum allowed

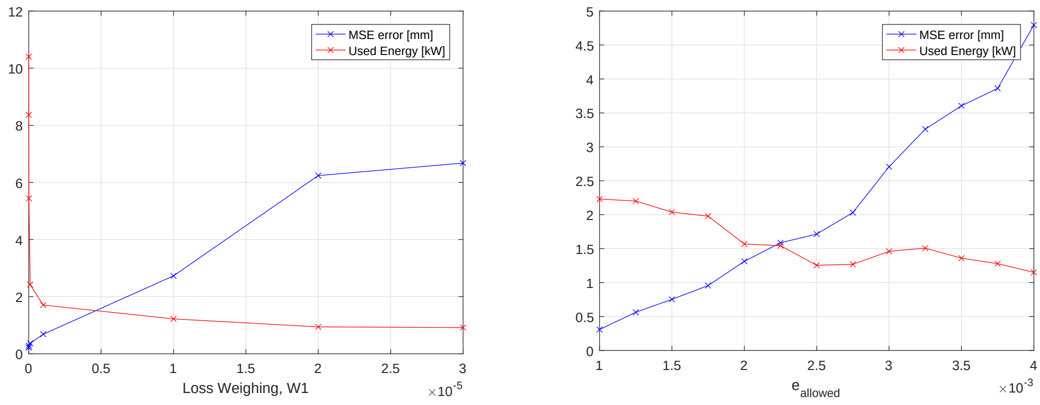

(a) (b)

Figure 7: Energy and mean squared error with various weighing parameters and allowed error on MPC_1 and MPC_2 respectively.

tracking error of (6) is shown. Tracking error is seen to increases with the allowed error while the energy loss decreases.

In Fig. 8 the weight on the energy loss in the FSA for the PID controller is varied. The allowed shifting time is chosen to 50ms due to the actuator dynamics.

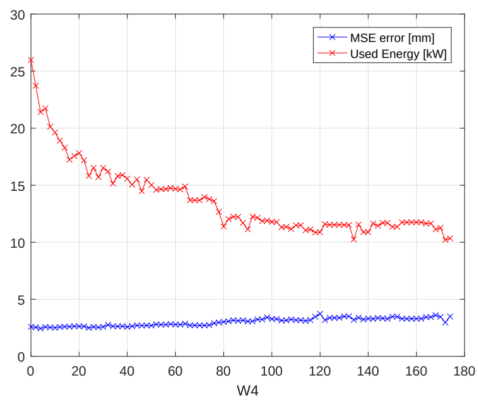

Figure 8: Energy and mean squared error for PID with various weights on energy loss.

As seen the used energy decreases with the increased weighing while the mean squared tracking error increases. To compare the two MPC formulations given by (5) and (6) and the PID controller (19) each control strategy is tuned in order to meet a set criteria of maximum 3mm mean squared error over the trajectory. Fig. 9 shows the results when using the tuned controllers.

As seen both MPC formulations consume less energy compared to the PID controller. In Tab. 3 the controllers in Fig. 9 are compared along with controllers with different weightings. The time horizon and step time is chosen as 0.5s and 0.1s respectively for all MPC formulations.

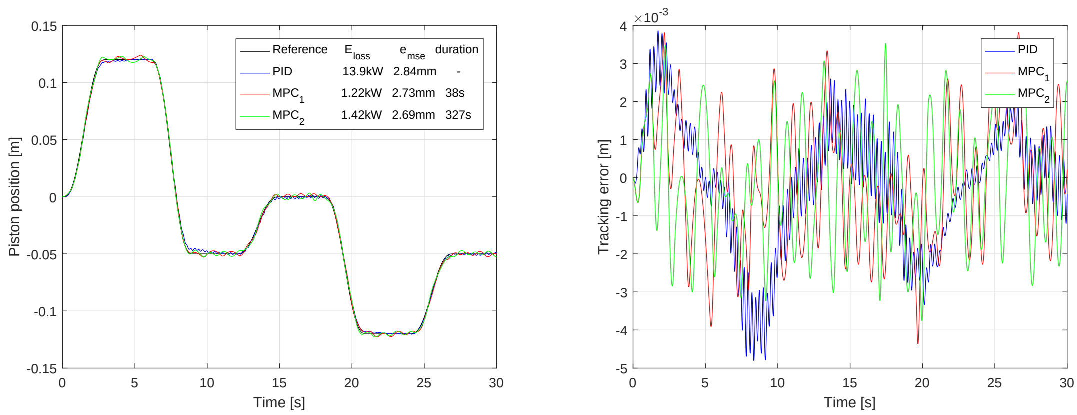

(a) (b)

Figure 9: Comparison of position tracking results the developed controllers.

	W_1	W_4	δ	E_{used}	e_{rms}	$e_{\max}$	N_{shift}
MPC_1	0	-	-	10.40kW	0.22mm	1.2mm	201
MPC_1^*	1e-5	-	-	1.22kW	2.73mm	3.8mm	71
MPC_1	5e-5	-	-	0.86kW	12.75mm	9.3mm	42
MPC_2	-	-	1mm	2.43kW	0.35mm	1.4mm	138
MPC_2^*	-	-	3mm	1.42kW	2.69mm	3.3mm	73
MPC_2	-	-	5mm	1.07kW	7.67mm	5.5mm	52
PID	-	0	-	24.05kW	2.62mm	3.2mm	496
PID*	-	75	-	13.86kW	2.84mm	3.9mm	439
PID	-	180	-	11.34kW	3.78mm	5.7mm	411

Table 3: Comparison of MPC_1(5), MPC_2(6) and PID (19) with different weightings. The * marked are the ones shown in Fig. 9.

4 DISCUSSION

The obtainable tracking precision is largely dependent on the force system configuration and the force system dynamics. The force step size entails the steady state position step, while a position value between the steady state values is obtained by modulating an actuator force between two force levels. During force modulation the time between force shifts dictates the position ripple which inevitably will appear when pulse modulating. Hence, reducing the step time improves the obtainable tracking precision, however, as seen in Fig. 6 decreasing the time step to improve the tracking is likely to increase the energy use.

How fast the actual force may change is limited by the pressure shifts in the individual cylinder chambers.

A final factor to include in choice of time step is the calculation time for the controller. The PID is very light in calculation time while the MPC is rather heavy on calculation time. The MPC algorithm performs an optimisation at each time step, and therefore, the optimisation routine is required to finish within T_s. The calculation time of the MPC algorithm is significantly dependent on the number of design variables for the optimisation routine (the combination of time step and prediction horizon). Furthermore, the complexity of the model used in the MPC algorithm affects the calculation time. As the current study is solely a simulation study calculation time is of less importance. However, the mean calculation time for one time step optimisation is around 38s and 327s for the two MPC algorithms shown in Fig. 9.

With the time step and the prediction horizon set the tuning of the MPC algorithms is done by choosing the weighing parameter W_1 and the tracking error measure δ for MPC_1 and MPC_2 respectively. For MPC_1 the weighing parameter is rather difficult directly to relate to system performance, contrary the δ value for the MPC_2 algorithm is directly associated with the position error. Hence, given a position tracking demand the MPC_2 algorithm is easily tuned to obey the demands while minimising energy use.

Stability analysis of the MPC algorithms studied is left untreated in this study, but, as mentioned a velocity error was included in MPC_1 to obtain a stable solution. Future studies should seek to prove stability of the designed algorithms.

Comparing the number of force shifts performed (last column in table 3) it is seen that the PID controller executes significantly more force shifts and uses a lot more energy than the MPC algorithms. It was observed that increasing the weighing parameter W_4 further may decrease the energy use, however leading to the PID algorithm performing almost no force shifts leading to a very poor position tracking. Improving the energy performance of the PID algorithm should, if required, instead be accomplished by increasing the step time even though this likewise leads to weaker position tracking.

For a steady state position reference the required force is a pulse modulation of two forces, but it is difficult to locate the optimal force trajectory. For example: *Let the position reference be x_r which impose a force that is pulse width modulated with duty cycle 0.4 between forces F_3 and F_4, with solution $f(t)$ leading to e_x a solution with the same position tracking is obtained by time shifting the PWM signal.* Hence, with the MPC structures applied the optimisation algorithm may have difficulty in differing various solutions especially for steady state input references.

5 CONCLUSSION

The current feasibility study indicates that MPC may be utilised for energy optimal tracking control with a discrete displacement cylinder. Bearing in mind that the study is merely a simulation study it is shown that a MPC algorithm may be designed for a discrete displacement cylinder such that an energy optimal position tracking is performed. The study shows that a MPC strategy including the discrete nature and simple loss models of the actuation system easily outperforms a PID controller combined with a force shifting algorithm.

Two MPC algorithms resulting in almost equal performance were developed. The MPC_2 algorithm seems more intuitive and simpler to tune. A parameter study showed that a relatively good performance may be obtained using a relative short prediction horizon, $T_\text{H} = 0.5s$, and sample time, $T_\text{s} = 0.1s$.

In conclusion, a MPC algorithm can be used to improve the energy efficiency of discrete displacement cylinder drives doing tracking control, if system model including energy losses may be developed such the optimisation routine can be executed in due time.

References

[1] M Linjama, Mr. H-P Vihtanen, Mr. A Sipola, Prof. M Vilenius: *Secondary Controlled Multi-Chamber Hydraulic Cylinder* In proceedings of The 11th Scandinavian International Conference on Fluid Power, SICFP09, June 2-4, 2009, Linkping, Sweden

[2] Mikko Huova, Arttu Aalto, Matti Linjama, Kalevi Huhtala, Tapio Lantela & Matti Pietola: *Digital hydraulic multi-pressure actuator the concept, simulation study and first experimental results* International Journal of Fluid Power 2017, ISSN: 1439-9776 (Print) 2332-1180 (Online), DOI: 10.1080/14399776.2017.1302775

[3] Rico H. Hansen, Torben O. Andersen and Henrik C. Pedersen: *Analysis of Discrete Pressure Level Systems for Wave Energy Converters* In proceedings of 2011 International Conference on Fluid Power and Mechatronics, DOI: 10.1109/FPM.2011.6045825

[4] Rico H. Hansen, Morten M. Kramer and Enrique Vidal: *Discrete Displacement Hydraulic Power Take-Off System for the Wavestar Wave Energy Converter* Energies 2013, 6, 4001-4044; doi:10.3390/en6084001

[5] Anders Hedegaard Hansen and Henrik C. Pedersen: *Optimal configuration of a discrete fluid power force system utilised in the PTO for WECs* Ocean Engineering 117(2016)8898, https://doi.org/10.1016/j.oceaneng.2016.03.032

[6] Anders Hedegaard Hansen and Henrik C. Pedersen: *Reducing pressure oscillations in discrete fluid power systems* Proc IMechE Part I: J Systems and Control Engineering, DOI: 10.1177/0959651815625015

[7] Rico H. Hansen, Torben O. Andersen, Henrik C. Pedersen and Anders H. Hansen: *Control of a 420 kN Discrete Displacement Cylinder Drive for the Wavestar Wave Energy Converter* In Proceedings of the ASME/BATH 2014 Symposium on Fluid Power & Motion Control, FPMC 2014, September 10 - 12, 2014, Bath, UK, FPMC2014-7833

[8] Anders Hedegaard Hansen, Henrik C. Pedersen and Rico Hjerm Hansen: *Validation of Simulation Model for Full Scale Wave Simulator and Discrete Fuild Power PTO System* Proceedings of the 9th JFPS International Symposium on Fluid Power, Matsue, 2014, Oct. 28 - 31, 2014

[9] Herbert Merritt: *Hydraulic Control Systems* John Wiley & sons, 1967. ISBN: 0 471 59617 5

[10] Michael M. Bech, Christian Noergaard, Daniel B. Roemer andSaku Kukkonen *A Global Multi-Objective Optimization Tool for Design of Mechatronic Components using Generalized Differential Evolution* Proceedings of the 42nd Annual Conference of IEEE Industrial Electronics Society, IECON 2016 ISBN:978-1-5090-3474-1